



Received 2 February 2019

Accepted 15 May 2019

Edited by Y. Amemiya, University of Tokyo,
Japan

Keywords: ellipsoidal mirror; soft X-ray
free-electron laser; saturable absorption;
optical design.

Intense sub-micrometre focusing of soft X-ray free-electron laser beyond $10^{16} \text{ W cm}^{-2}$ with an ellipsoidal mirror

Hiroto Motoyama,^{a*} Shigeki Owada,^{b,c} Gota Yamaguchi,^d Takehiro Kume,^d Satoru Egawa,^d Kensuke Tono,^{b,c} Yuichi Inubushi,^{b,c} Takahisa Koyama,^{b,c} Makina Yabashi,^{b,c} Haruhiko Ohashi^{b,c} and Hidekazu Mimura^d

^aDepartment of Chemistry, School of Science, The University of Tokyo, 7-3-1 Hongo, Bunkyo, Tokyo 113-8656, Japan, ^bRIKEN Spring-8 Center, 1-1-1 Koto, Sayo-cho, Sayo-gun, Hyogo 679-5148, Japan, ^cJapan Synchrotron Radiation Research Institute, 1-1-1 Koto, Sayo-cho, Sayo-gun, Hyogo 679-5198, Japan, and ^dDepartment of Precision Engineering, School of Engineering, The University of Tokyo, 7-3-1 Hongo, Bunkyo, Tokyo 113-8656, Japan.

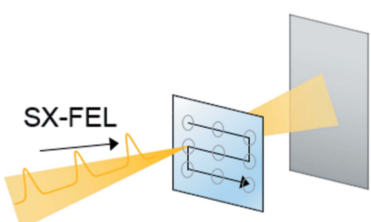
*Correspondence e-mail: motoyama@chem.s.u-tokyo.ac.jp

Intense sub-micrometre focusing of a soft X-ray free-electron laser (FEL) was achieved by using an ellipsoidal mirror with a high numerical aperture. A hybrid focusing system in combination with a Kirkpatrick–Baez mirror was applied for compensation of a small spatial acceptance of the ellipsoidal mirror. With this system, the soft X-ray FEL pulses were focused down to $480 \text{ nm} \times 680 \text{ nm}$ with an extremely high intensity of $8.8 \times 10^{16} \text{ W cm}^{-2}$ at a photon energy of 120 eV, which yielded saturable absorption at the *L*-edge of Si (99.8 eV) with a drastic increase of transmittance from 8% to 48%.

1. Introduction

X-ray free-electron lasers (XFELs) have produced femtosecond X-ray pulses (Emma *et al.*, 2010; Ishikawa *et al.*, 2012; Shintake *et al.*, 2008; Ackermann *et al.*, 2007; Allaria *et al.*, 2012; Kang *et al.*, 2017; Milne *et al.*, 2017; Tschentscher *et al.*, 2017) with high intensity, which can be further enhanced by using a focusing optical system. For the hard X-ray region, total reflection optics in the Kirkpatrick–Baez (KB) configuration (Kirkpatrick & Baez, 1948), which consists of a pair of one-dimensional grazing-incidence elliptical mirrors, have been widely utilized due to their high damage threshold and high reflectivity in a wide range of photon energies (Boutet & Williams, 2010; Yumoto *et al.*, 2012; Mimura *et al.*, 2014; Kim *et al.*, 2018; Matsuyama *et al.*, 2018). By tightly focusing hard X-rays, ultra-intense X-ray light fields can be generated, promoting research into nonlinear X-ray optics, such as X-ray two-photon absorption (Tamasaku *et al.*, 2014, 2018; Ghimire *et al.*, 2016), saturable absorption of X-rays (Yoneda *et al.*, 2014; Rackstraw *et al.*, 2015) and lasing from an atomic inner shell (Rohringer *et al.*, 2012; Yoneda *et al.*, 2015).

For focusing of soft X-ray FELs, the KB configuration has been widely employed (Owada *et al.*, 2018; Dzirzhitski *et al.*, 2016; Schlotter *et al.*, 2012). However, it is more difficult to achieve a small focus in the longer wavelength regime, because the surface profile becomes much steeper under a higher incident angle required for a higher numerical aperture (NA) condition. Typical focus sizes are currently limited from one to several micrometres. A multilayered normal-incidence mirror in a single-reflection geometry was developed for sub-micrometre focusing with an intensity of $10^{16} \text{ W cm}^{-2}$ (Nelson *et al.*, 2009), which enabled the observation of saturable absorption



© 2019 International Union of Crystallography

in solid aluminium (Nagler *et al.*, 2009). The normal-incidence mirror has a large numerical aperture and large acceptance, but the multilayered structure imposes a limitation on the wavelength to be applicable.

Recently, we have developed a new scheme to produce high-quality grazing-incidence ellipsoidal mirrors, where a two-dimensional focus is generated with a single optical device. The single reflection geometry provides the advantage of short focal lengths in both the vertical and horizontal directions so as to produce a small focus. Furthermore, an alignment procedure becomes straightforward with a simpler mirror manipulator system. In order to fabricate high-NA ellipsoidal mirrors with a steep surface profile, a two-step fabrication process was developed. A precise quartz mandrel, which has an ellipsoidal surface, is first fabricated (Takei & Mimura, 2017), and the shape of the mandrel is replicated to a thick nickel layer by means of a room-temperature electro-forming process (Kume *et al.*, 2014). The figure error of the mandrel was ~ 20 nm peak-to-valley, which is sufficiently low for reflecting soft X-rays with a wavelength around 10 nm. A nickel surface has a broadband reflectance for the wavelength ranging from 10 nm to 30 nm (Henke *et al.*, 1993). With this process, we were able to suppress the wavefront error below $\lambda/4$, and produce a sub-micrometre focusing spot for broadband high-order harmonics in the extreme ultraviolet (EUV) region ($\lambda = 10\text{--}20$ nm; Motoyama *et al.*, 2019) and for soft X-ray synchrotron radiation ($\lambda = 4$ nm; Mimura *et al.*, 2018).

In this report, we describe a focusing system with an ellipsoidal mirror for sub-micrometre focusing of soft X-ray FEL pulses with high efficiency. Since the spatial acceptance of the ellipsoidal mirror fabricated with the present process is limited to a few millimetres, being smaller than the typical size of the unfocused soft X-ray FEL beam, we combined a KB mirror system as the prefocusing optics to match the incident beam size with the acceptance of the ellipsoidal mirror. We constructed this hybrid two-stage focusing system at the soft X-ray FEL beamline (BL1) of SACLAs (Owada *et al.*, 2018), and produced a $480\text{ nm} \times 680\text{ nm}$ focus with an extremely high intensity of $8.8 \times 10^{16}\text{ W cm}^{-2}$ at a photon energy of 120 eV. Saturable absorption in Si_3N_4 thin film was successfully observed.

Table 1
Parameters of the KB mirror system and ellipsoidal mirror.

	KB mirror system (Owada <i>et al.</i> , 2018)	Ellipsoidal mirror
Mirror size	Length: 600 mm Width: 50 mm	Length: 50 mm Upstream diameter: 12 mm Downstream diameter: 5 mm
Surface material	Carbon	Nickel
Glancing angle	~ 26 mrad	(max) 140 mrad
Spatial acceptance	15 mm	3.5 mm
Focal length	(Horizontal) 2.65 m (Vertical) 2.0 m	35 mm

2. Optical configuration

Fig. 1 shows the optical configuration. The incident beam is prefocused using a KB system with a focal length of 2000 mm, which was installed at SACLAs BL1 as a common-use microfocusing device with a high reflectivity for wavelengths longer than 4.4 nm (Owada *et al.*, 2018). The detailed parameters of the elliptical mirror are listed in Table 1. The ellipsoidal mirror is located 500 mm downstream from the KB focus. Here the beam size is reduced to 2.5 mm in $1/e^2$ width, which is a quarter of the size of the incident beam to the KB system, so as to match the spatial acceptance of the ellipsoidal mirror.

In the optical design of the ellipsoidal mirror, a higher glancing incident angle is preferable for increasing NA, although careful investigation is required to avoid surface damage with the intense soft X-ray FEL pulse under the higher incident-angle condition with larger absorption (Khorsand *et al.*, 2010; Hau-Riege *et al.*, 2007; Kim *et al.*, 2013; Koyama *et al.*, 2013). Before we fabricated the ellipsoidal mirror, we checked the damage threshold of a nickel-coated silicon wafer by irradiating 10 000 shots at different incident angles: 140 mrad, 280 mrad and 1.52 rad (normal incidence), as shown in Fig. 2(a). In the damage test, the soft XFEL pulses, focused by the KB system, were irradiated on the sample as shown in Fig. 1. The surface morphology of the irradiated position was observed with a white-light interferometer to determine the damage threshold. As shown in Fig. 2(b), the damage thresholds determined show a good agreement with the calculated value under the assumption that a single pulse is

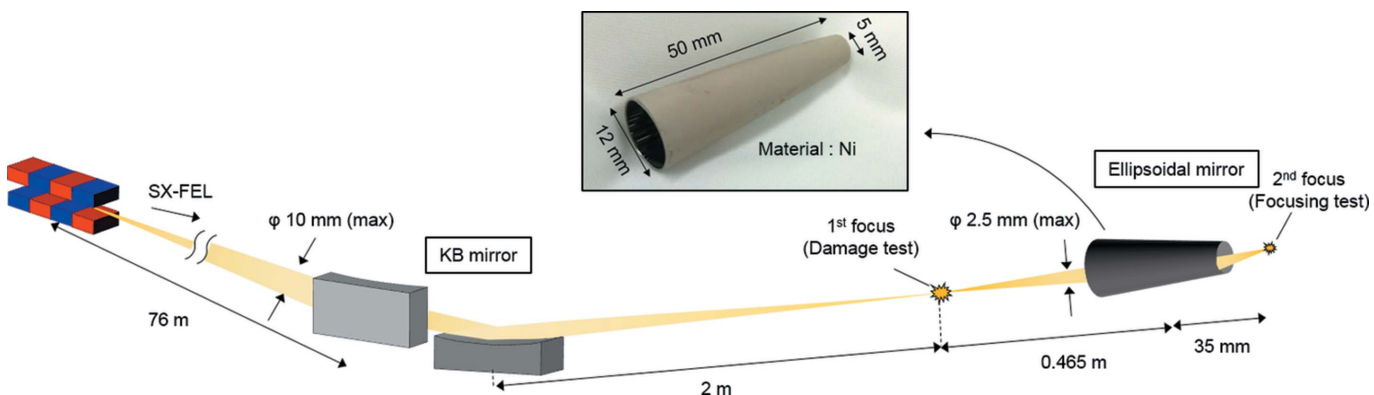
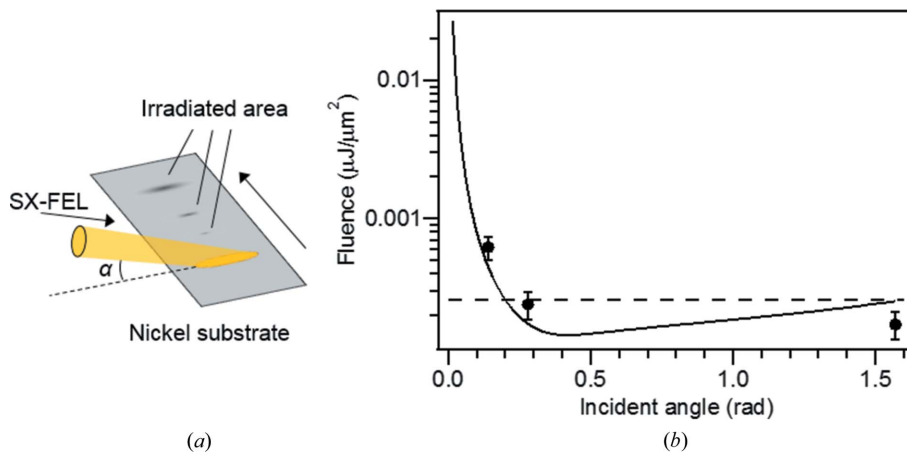


Figure 1

Optical configuration. The soft X-ray FEL beam is first focused by the KB mirror system and refocused by the ellipsoidal mirror. The incident beam size to the ellipsoidal mirror is a quarter of the initial size. The system was installed at the soft XFEL beamline (BL1) of SACLAs.

**Figure 2**

Determination of damage threshold by irradiating the soft XFEL pulses. (a) Schematic of the experimental setup. Multiple positions on the nickel-coated substrate were irradiated by 10 000 shots of soft XFEL pulses with different average intensity. (b) Damage threshold plotted as a function of the glancing incident angle. Filled circles are experimentally determined values and the solid line is a calculated curve for the single-shot damage threshold. The error bars are the $\pm 2\sigma$ of the fluence fluctuation of the incident soft XFEL pulses. The dashed line indicates an estimated fluence value ($0.26 \times 10^{-3} \mu\text{J } \mu\text{m}^{-2}$) when the soft XFEL beam (200 μJ , diameter 1 mm) irradiates the surface.

incident on the surface. The dotted line indicates the fluence when the soft X-ray pulse with a pulse energy of 200 μJ and a diameter of 1 mm irradiates the sample. This fluence is considered to be the upper limit in our experimental system at the BL1 of SACLA. The damage threshold should be higher than this value to avoid damage on the mirror surface. We set the maximum glancing incident angle (θ_{\max}) to be 140 mrad, at which the damage threshold is sufficiently higher than the fluence experienced by the ellipsoidal mirror.

The length of the ellipsoidal mirror is designed to be 50 mm by considering the capability of the present fabrication process. The working distance is set to be 10 mm. When the center of the mirror is illuminated, the numerical aperture is approximately given by

$$\text{NA} = \frac{2.35D/8}{f + l/2},$$

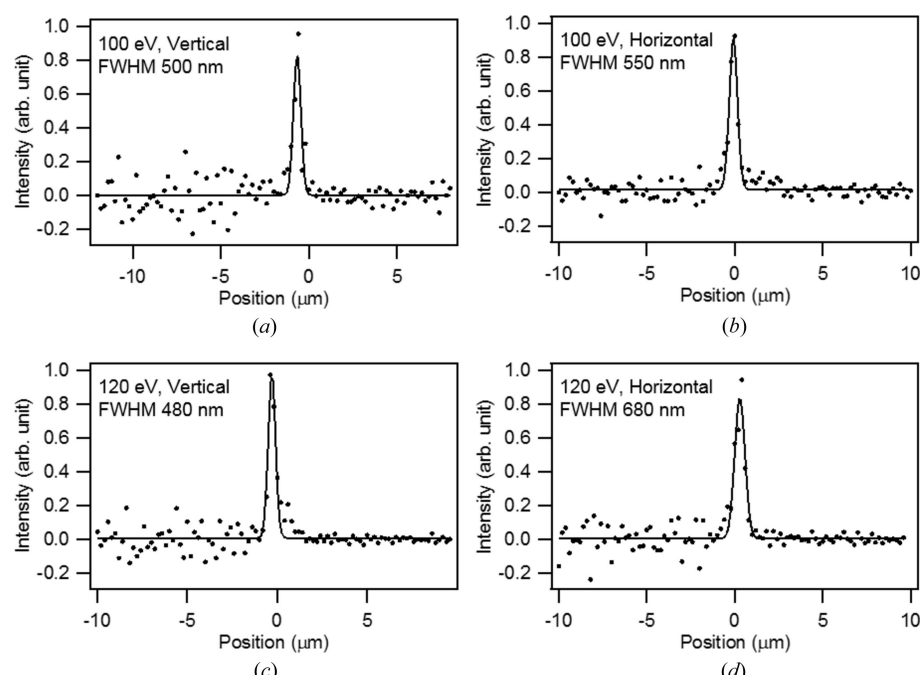
where D , l and f are the diameter of the incident beam in $1/e^2$ width, the length of the mirror and working distance, respectively. A diffraction-limited focusing size, given by $0.62\lambda/\text{NA}$, is evaluated to be ~ 370 nm at a wavelength (λ) of 12.4 nm and D of 2.5 mm. The distance (L) from the KB focus to the final focus is 500 mm. With the parameters L , f and θ_{\max} , we were able to determine the surface profile of the ellipsoidal mirror including the lengths of the major and minor axes. The spatial acceptance of the ellipsoidal mirror is

designed to be ~ 3.5 mm, which is larger than D at a photon energy of 100 eV ($\lambda = 12.4$ nm). The parameters of the ellipsoidal mirror are listed in Table 1.

3. Characterization of the focused beam

The experiment was performed at BL1 of SACLA, with photon energies of 100 eV ($\lambda = 12.4$ nm) and 120 eV ($\lambda = 10.3$ nm). The KB system was aligned to obtain a focus of $\sim 10 \mu\text{m} \times 10 \mu\text{m}$. At the final focus of the ellipsoidal mirror, two knife-edges are installed for performing a Foucault test and a knife-edge scan in both the vertical and horizontal directions. The beam profiles and the intensity of the reflected beam were measured with a multi-channel plate coupled with a phosphor screen. The ellipsoidal mirror is aligned with a five-axis mirror manipulator consisting of piezo electric stages that provide a rotation resolution of ~ 1.0 μrad .

Fig. 3 shows focused beam profiles measured in the vertical and horizontal directions at different photon energies of 100 eV and 120 eV. We found that the focused beam sizes defined as the full width at half-maxima were 500 nm \times 550 nm and 480 nm \times 680 nm at photon energies of 100 eV and 120 eV, respectively. In addition, the focusing system can

**Figure 3**

Intensity profile of the focused soft XFEL pulses measured at photon energies of 100 eV in (a) the vertical and (b) the horizontal direction, and 120 eV in (c) the vertical and (d) the horizontal direction. The circular dots are experimentally obtained data; the solid line is a fitted curve with Gaussian function.

stably produce a sub-micrometre beam over at least 6 h without realignment of the mirror.

4. Saturable absorption in the Si_3N_4 membrane

Assuming the typical pulse energy and pulse duration of the soft X-ray pulses available at BL1, the power density at the focus is estimated to be higher than $10^{16} \text{ W cm}^{-2}$. The material placed in such an extremely intense soft X-ray field becomes optically transparent; this is called a saturable absorption. To date, the saturable absorption of Sn in the EUV region (Yoneda *et al.*, 2009), Al in the soft X-ray region (Nagler *et al.*, 2009), and Fe and Cu in the hard X-ray region (Yoneda *et al.*, 2014, 2015) have been reported. The observation of saturable absorption is evidence of the generation of extreme and intense power density.

Using the present focusing system, we irradiated a 150 nm-thick Si_3N_4 membrane by a nano-focused soft XFEL pulse. To excite the *L*-shell electron of Si ($h\nu = 99.8 \text{ eV}$) with a single photon, the photon energy of soft XFEL was tuned to 120 eV. The beam intensity after the sample is measured with a photodiode covered with a 200 nm-thick Zr filter that eliminates the stray visible light. The pulse energy was controlled by the gas attenuator filled with Ar. Since the estimated atomic dose at the sample ranges from 20 eV per atom to 60 000 eV per atom, the position of the sample was transversely moved for every transmission measurement as shown in Fig. 4(a).

The minimum number of photons (N_p) required for saturable absorption can be roughly estimated considering the number of Si atoms in which the focused beam propagates, absorbance of the FEL to excite *L*-shell electrons, pulse duration of the FEL pulse and lifetime of *L*-shell vacancy. In our experimental systems, the threshold of peak intensity for saturable absorption is estimated to be $\sim 8.0 \times 10^{14} \text{ W cm}^{-2}$, which can be achieved with our focusing system.

The transmittance measured through the Si_3N_4 membrane is plotted as a function of a peak intensity in Fig. 4(b). Each data point in Fig. 4(b) is derived from a single-shot measurement. A peak intensity is calculated assuming that the pulse

duration is 100 fs (Kubota *et al.*, 2019; Owada *et al.*, 2019; Harries *et al.*, 2018). The transmission measured with low peak intensities as a reference value was only 8%. However, the transmission drastically increased with higher peak intensity beyond $10^{15} \text{ W cm}^{-2}$, and finally reached 48% at the highest available peak intensity of $8.8 \times 10^{16} \text{ W cm}^{-2}$. In addition, the peak intensity at which the transmission starts to increase is consistent with the estimated value in the previous paragraph. The capability for generating extremely intense soft X-ray laser fields was proven through observation of the saturable absorption.

5. Discussion

The hybrid soft XFEL focusing system, which combined the KB system with the ellipsoidal mirror, was designed and demonstrated at BL1 of SACLAs. We achieved focusing of the soft XFEL beam down to a sub-1 μm spot. The intense nano-focused beam produced by this system induced the saturable absorption of the *L*-edge of Si (99.8 eV) with an incident photon energy of 120 eV.

Owing to a broadband reflectance of the focusing optics, the system is available for investigation of nonlinear optical responses of various materials with *M*- or *L*-edge binding energies in the 50 eV to 150 eV range such as Fe, Ni and Cu as well as Si. In addition to the high peak intensity, a spatial resolution can be better than 1 μm for scanning microscopic experiments. We emphasize that the nano-focusing system could be readily realized by placing the present ellipsoidal mirror at a position downstream of the existing focusing system.

Acknowledgements

The authors thank the SACLAs engineering team for their help during the beam time.

Funding information

This work was supported by the SACLAs Research Support Program for Graduate Students and JSPS KAKENHI (grant Nos. JP15J08622 and JP15H02041).

References

- Ackermann, W., Asova, G., Ayvazyan, V., Azima, A., Baboi, N., Bähr, J., Balandin, V., Beutner, B., Brandt, A., Bolzmann, A., Brinkmann, R., Brovko, O. I., Castellano, M., Castro, P., Catani, L., Chiadroni, E., Choroba, S., Cianchi, A., Costello, J. T., Cubaynes, D., Dardis, J., Decking, W., Delsim-Hasheemi, H., Delserieys, A., Di Pirro, G., Dohlus, M., Düsterer, S., Eckhardt, A., Edwards, H. T., Faatz, B., Feldhaus, J., Flöttmann, K., Frisch, J., Fröhlich, L., Garvey, T., Gensch, U., Gerth, C., Görler, M., Golubeva, N., Grabosch, H.-J., Grecki, M., Grimm, O., Hacker, K., Hahn, U., Han, J. H., Honkavaara, K., Hott, T., Hüning, M.,

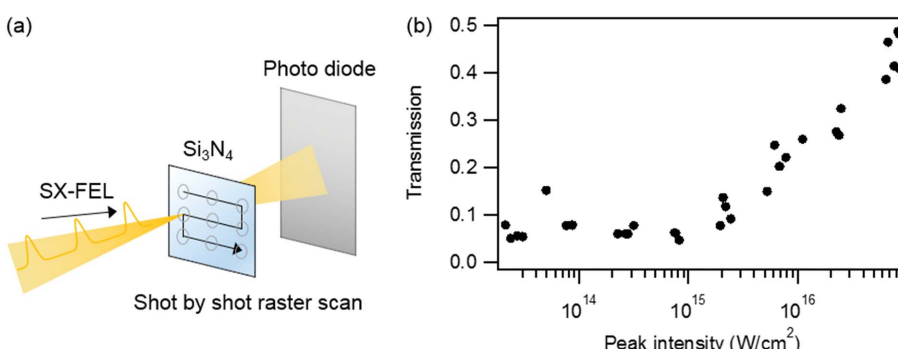


Figure 4

Saturable absorption of an Si_3N_4 membrane induced by a focused soft XFEL pulse. (a) Schematic of the experimental setup. The single nano-focused soft XFEL pulse was focused on the 150 nm-thick Si_3N_4 membrane. The intensity of the transparent light was measured using a photodiode. (b) Transmission of the nano-focused beam plotted as a function of the intensity for 120 eV.

- Ivanisenko, Y., Jaeschke, E., Jalmuzna, W., Jezynski, T., Kammering, R., Katalev, V., Kavanagh, K., Kennedy, E. T., Khodyachykh, S., Klose, K., Kocharyan, V., Körfer, M., Kollewe, M., Koprek, W., Korepanov, S., Kostin, D., Krassilnikov, M., Kube, G., Kuhlmann, M., Lewis, C. L. S., Lilje, L., Limberg, T., Lipka, D., Löhl, F., Luna, H., Luong, M., Martins, M., Meyer, M., Michelato, P., Miltchev, V., Möller, W. D., Monaco, L., Müller, W. F. O., Napieralski, O., Napol, O., Nicolosi, P., Nölle, D., Nuñez, T., Oppelt, A., Pagani, C., Paparella, R., Pchalek, N., Pedregosa-Gutierrez, J., Petersen, B., Petrosyan, B., Petrosyan, G., Petrosyan, L., Pflüger, J., Plönjes, E., Poletto, L., Pozniak, K., Prat, E., Proch, D., Pucyk, P., Radcliffe, P., Redlin, H., Rehlich, K., Richter, M., Roehrs, M., Roensch, J., Romaniuk, R., Ross, M., Rossbach, J., Rybnikov, V., Sachwitz, M., Saldin, E. L., Sandner, W., Schlarb, H., Schmidt, B., Schmitz, M., Schmüser, P., Schneider, J. R., Schneidmiller, E. A., Schnepf, S., Schreiber, S., Seidel, M., Sertore, D., Shabunov, A. V., Simon, C., Simrock, S., Sombrowski, E., Sorokin, A. A., Spanknebel, P., Spesvtsev, R., Staykov, L., Steffen, B., Stephan, F., Stulle, F., Thom, H., Tiedtke, K., Tischer, M., Toleikis, S., Treusch, R., Trines, D., Tsakov, I., Vogel, E., Weiland, T., Weise, H., Wellhöfer, M., Wendt, M., Will, I., Winter, A., Wittenburg, K., Wurth, W., Yeates, P., Yurkov, M. V., Zagorodnov, I. & Zapfe, K. (2007). *Nat. Photon.* **1**, 336–342.
- Allaria, E., Appio, R., Badano, L., Barletta, W. A., Bassanese, S., Biedron, S. G., Borga, A., Busetto, E., Castronovo, D., Cinquegrana, P., Cleva, S., Cocco, D., Cornacchia, M., Craievich, P., Cudin, I., D'Auria, G., Dal Forno, M., Danailov, M. B., De Monte, R., De Ninno, G., Delgiusto, P., Demidovich, A., Di Mitri, S., Diviacco, B., Fabris, A., Fabris, R., Fawley, W., Ferianis, M., Ferrari, E., Ferry, S., Froehlich, L., Furlan, P., Gaio, G., Gelmetti, F., Giannessi, L., Giannini, M., Gobessi, R., Ivanov, R., Karantzoulis, E., Lonza, M., Lutman, A., Mahieu, B., Milloch, M., Milton, S. V., Musardo, M., Nikolov, I., Noe, S., Parmigiani, F., Penco, G., Petronio, M., Pivetta, L., Predonzani, M., Rossi, F., Rumiz, L., Salom, A., Scafuri, C., Serpico, C., Sigalotti, P., Spampinati, S., Spezzani, C., Svandrlík, M., Svetina, C., Tazzari, S., Trovo, M., Ümer, R., Vascotto, A., Veronese, M., Visintini, R., Zaccaria, M., Zangrandino, D. & Zangrandino, M. (2012). *Nat. Photon.* **6**, 699–704.
- Boutet, S. & Williams, J. (2010). *New J. Phys.* **12**, 035024.
- Dziarzyński, S., Gerasimova, N., Goderich, R., Mey, T., Reininger, R., Rübhausen, M., Siewert, F., Weigelt, H. & Brenner, G. (2016). *J. Synchrotron Rad.* **23**, 123–131.
- Emma, P., Akre, R., Arthur, J., Bionta, R., Bostedt, C., Bozek, J., Brachmann, A., Bucksbaum, P., Coffee, R., Decker, F.-J., Ding, Y., Dowell, D., Edstrom, S., Fisher, A., Frisch, J., Gilevich, S., Hastings, J., Hays, G., Hering, P., Huang, Z., Iverson, R., Loos, H., Messerschmidt, M., Miahnahri, A., Moeller, S., Nuhn, H.-D., Pile, G., Ratner, D., Rzepliela, J., Schultz, D., Smith, T., Stefan, P., Tompkins, H., Turner, J., Welch, J., White, W., Wu, J., Yocky, G. & Galayda, J. (2010). *Nat. Photon.* **4**, 641–647.
- Ghimire, S., Fuchs, M., Hastings, J., Herrmann, S. C., Inubushi, Y., Pines, J., Schwartz, S., Yabashi, M. & Reis, D. A. (2016). *Phys. Rev. A*, **94**, 1–6.
- Harries, J. R., Iwayama, H., Kuma, S., Iizawa, M., Suzuki, N., Azuma, Y., Inoue, I., Owada, S., Togashi, T., Tono, K., Yabashi, M. & Shigemasa, E. (2018). *Phys. Rev. Lett.* **121**, 263201.
- Hau-Riege, S. P., London, R. A., Bionta, R. M., McKernan, M. A., Baker, S. L., Krzywinski, J., Sobierajski, R., Nietubyc, R., Pelka, J. B., Jurek, M., Juha, L., Chalupský, J., Čihelka, J., Hájková, V., Velyhan, A., Krásá, J., Kuba, J., Tiedtke, K., Toleikis, S., Tschentscher, T., Wabnitz, H., Bergh, M., Caleman, C., Sokolowski-Tinten, K., Stojanovic, N. & Zastraub, U. (2007). *Appl. Phys. Lett.* **90**, 11–14.
- Henke, B. L., Gullikson, E. M. & Davis, J. C. (1993). *At. Data Nucl. Data Tables*, **54**, 181–342.
- Ishikawa, T., Aoyagi, H., Asaka, T., Asano, Y., Azumi, N., Bizen, T., Ego, H., Fukami, K., Fukui, T., Furukawa, Y., Goto, S., Hanaki, H., Hara, T., Hasegawa, T., Hatsui, T., Higashiyama, A., Hiroto, T., Hosoda, N., Ishii, M., Inagaki, T., Inubushi, Y., Itoga, T., Joti, Y., Kago, M., Kameshima, T., Kimura, H., Kirihara, Y., Kiyomichi, A., Kobayashi, T., Kondo, C., Kudo, T., Maesaka, H., Maréchal, X. M., Masuda, T., Matsubara, S., Matsumoto, T., Matsushita, T., Matsui, S., Nagasano, M., Nariyama, N., Ohashi, H., Ohata, T., Ohshima, T., Ono, S., Otake, Y., Saji, C., Sakurai, T., Sato, T., Sawada, K., Seike, T., Shirasawa, K., Sugimoto, T., Suzuki, S., Takahashi, S., Takebe, H., Takeshita, K., Tamasaku, K., Tanaka, H., Tanaka, R., Tanaka, T., Togashi, T., Togawa, K., Tokuhisa, A., Tomizawa, H., Tono, K., Wu, S., Yabashi, M., Yamaga, M., Yamashita, A., Yanagida, K., Zhang, C., Shintake, T., Kitamura, H. & Kumagai, N. (2012). *Nat. Photon.* **6**, 540–544.
- Kang, H., Min, C., Heo, H., Kim, C., Yang, H., Kim, G., Nam, I., Baek, S. Y., Choi, H., Mun, G., Park, B. R., Suh, Y. J., Shin, D. C., Hu, J., Hong, J., Jung, S., Kim, S., Kim, K., Na, D., Park, S. S., Park, Y. J., Han, J., Jung, Y. G., Jeong, S. H., Lee, H. G., Lee, S., Lee, S., Lee, W., Oh, B., Suh, H. S., Parc, Y. W., Park, S., Kim, M. H., Jung, N., Kim, Y., Lee, M., Lee, B., Sung, C., Mok, I., Yang, J., Lee, C., Shin, H., Kim, J. H., Kim, Y., Lee, J. H., Park, S., Kim, J., Park, J., Eom, I., Rah, S., Kim, S., Nam, K. H., Park, J., Park, J., Kim, S., Kwon, S., Park, S. H., Kim, K. S., Hyun, H., Kim, S. N., Kim, S., Hwang, S., Kim, M. J., Lim, C., Yu, C., Kim, B., Kang, T., Kim, K., Kim, S., Lee, H., Lee, H., Park, K., Koo, T., Kim, D. & Ko, I. S. (2017). *Nat. Photon.* **11**, 708–713.
- Khorsand, A. R., Sobierajski, R., Louis, E., Bruijn, S., van Hattum, E. D., van de Kraij, R. W. E., Jurek, M., Klinger, D., Pelka, J. B., Juha, L., Burian, T., Chalupský, J., Čihelka, J., Hájková, V., Vysin, L., Jastrow, U., Stojanovic, N., Toleikis, S., Wabnitz, H., Tiedtke, K., Sokolowski-Tinten, K., Shymanovich, U., Krzywinski, J., Hau-Riege, S., London, R., Gleeson, A., Gullikson, E. M. & Bijkerk, F. (2010). *Opt. Express*, **18**, 700.
- Kim, J., Kim, H.-Y., Park, J., Kim, S., Kim, S., Rah, S., Lim, J. & Nam, K. H. (2018). *J. Synchrotron Rad.* **25**, 289–292.
- Kim, J., Koyama, T., Yumoto, H., Nagahira, A., Matsuyama, S., Sano, Y., Yabashi, M., Ohashi, H., Ishikawa, T. & Yamauchi, K. (2013). *Proc. SPIE*, **8848**, 88480S.
- Kirkpatrick, P. & Baez, A. V. (1948). *J. Opt. Soc. Am.* **38**, 766–774.
- Koyama, T., Yumoto, H., Senba, Y., Tono, K., Sato, T., Togashi, T., Inubushi, Y., Kim, J., Kimura, T., Matsuyama, S., Mimura, H., Yabashi, M., Yamauchi, K., Ohashi, H. & Ishikawa, T. (2013). *J. Phys. Conf. Ser.* **463**, 012043.
- Kubota, Y., Inoue, I., Togawa, K., Kinjo, R., Iwayama, H., Harries, J. R., Inubushi, Y., Owada, S., Tono, K., Tanaka, T., Hara, T. & Yabashi, M. (2019). *2018 16th International Conference on Megagauss Magnetic Field Generation and Related Topics (MEGAGAUS)*, 25–29 September 2018, Kashiwa, Japan. IEEE (doi:10.1109/MEGAGAUSS.2018.8722659).
- Kume, T., Egawa, S. & Mimura, H. (2014). *J. Japan Soc. Precis. Eng.* **80**, 956–960.
- Matsuyama, S., Inoue, T., Yamada, J., Kim, J., Yumoto, H., Inubushi, Y., Osaka, T., Inoue, I., Koyama, T., Tono, K., Ohashi, H., Yabashi, M., Ishikawa, T. & Yamauchi, K. (2018). *Sci. Rep.* **8**, 17440.
- Milne, C., Schietinger, T., Aiba, M., Alarcon, A., Alex, J., Anghel, A., Arsov, V., Beard, C., Beaud, P., Bettini, S., Bopp, M., Brands, H., Brönnimann, M., Brunnenkant, I., Calvi, M., Citterio, A., Craievich, P., Csatari Divall, M., Dällenbach, M., D'Amico, M., Dax, A., Deng, Y., Dietrich, A., Dinapoli, R., Divall, E., Dordevic, S., Ebner, S., Erny, C., Fitze, H., Flechsig, U., Follath, R., Frei, F., Gärtnert, F., Ganter, R., Garvey, T., Geng, Z., Gorgisyan, I., Gough, C., Hauff, A., Hauri, C., Hiller, N., Humar, T., Hunziker, S., Ingold, G., Ischebeck, R., Janousch, M., Juranić, P., Jurcevic, M., Kaiser, M., Kalantari, B., Kalt, R., Keil, B., Kittel, C., Knopp, G., Koprek, W., Lemke, H., Lippuner, T., Llorente Sancho, D., Löhl, F., Lopez-Cuenca, C., Märki, F., Marcellini, F., Marinkovic, G., Martiel, I., Menzel, R., Mozzanica, A., Nass, K., Orlandi, G., Ozkan Loch, C., Panepucci, E., Paralić, M., Patterson, B., Pedrini, B., Pedrozzini, M., Pollet, P., Pradervand, C., Prat, E., Radi, P., Raguin, J.-Y., Redford, S., Rehanek, J., Réhault, J., Reiche, S., Ringele, M., Rittmann, J.,

- Rivkin, L., Romann, A., Ruat, M., Ruder, C., Sala, L., Schebacher, L., Schilcher, T., Schlott, V., Schmidt, T., Schmitt, B., Shi, X., Stadler, M., Stigelin, L., Sturzenegger, W., Szlachetko, J., Thattil, D., Treyer, D., Trisorio, A., Tron, W., Vetter, S., Vicario, C., Voulot, D., Wang, M., Zamofing, T., Zellweger, C., Zennaro, R., Zimoch, E., Abela, R., Patthey, L. & Braun, H.-H. (2017). *Appl. Sci.* **7**, 720.
- Mimura, H., Takei, Y., Kume, T., Takeo, Y., Motoyama, H., Egawa, S., Matsuzawa, Y., Yamaguchi, G., Senba, Y., Kishimoto, H. & Ohashi, H. (2018). *Rev. Sci. Instrum.* **89**, 093104.
- Mimura, H., Yumoto, H., Matsuyama, S., Koyama, T., Tono, K., Inubushi, Y., Togashi, T., Sato, T., Kim, J., Fukui, R., Sano, Y., Yabashi, M., Ohashi, H., Ishikawa, T. & Yamauchi, K. (2014). *Nat. Commun.* **5**, 3539.
- Motoyama, H., Iwasaki, A., Takei, Y., Kume, T., Egawa, S., Sato, T., Yamanouchi, K. & Mimura, H. (2019). *Appl. Phys. Lett.* **114**, 241102.
- Nagler, B., Zastraub, U., Fäustlin, R. R., Vinko, S. M., Whitcher, T., Nelson, A. J., Sobierajski, R., Krzywinski, J., Chalupsky, J., Abreu, E., Bajt, S., Bornath, T., Burian, T., Chapman, H., Cihelka, J., Döppner, T., Düsterer, S., Dzelzainis, T., Fajardo, M., Förster, E., Fortmann, C., Galtier, E., Glenzer, S. H., Göde, S., Gregori, G., Hajkova, V., Heimann, P., Juha, L., Jurek, M., Khattak, F. Y., Khorsand, A. R., Klinger, D., Kozlova, M., Laarmann, T., Lee, H. J., Lee, R. W., Meiweis-Broer, K.-H., Mercere, P., Murphy, W. J., Przystawik, A., Redmer, R., Reinholz, H., Riley, D., Röpke, G., Rosmej, F., Saksl, K., Schott, R., Thiele, R., Tiggesbäumker, J., Toleikis, S., Tschentscher, T., Uschmann, I., Vollmer, H. J. & Wark, J. S. (2009). *Nat. Phys.* **5**, 693–696.
- Nelson, A. J., Toleikis, S., Chapman, H., Bajt, S., Krzywinski, J., Chalupsky, J., Juha, L., Cihelka, J., Hajkova, V., Vysin, L., Burian, T., Kozlova, M., Fäustlin, R. R., Nagler, B., Vinko, S. M., Whitcher, T., Dzelzainis, T., Renner, O., Saksl, K., Khorsand, A. R., Heimann, P. A., Sobierajski, R., Klinger, D., Jurek, M., Pelka, J., Iwan, B., Andreasson, J., Timneanu, N., Fajardo, M., Wark, J. S., Riley, D., Tschentscher, T., Hajdu, J. & Lee, R. W. (2009). *Opt. Express*, **17**, 18271–18278.
- Owada, S., Nakajima, K., Togashi, T., Katayama, T., Yumoto, H., Ohashi, H. & Yabashi, M. (2019). *J. Synchrotron Rad.* **26**, 887–890.
- Owada, S., Togawa, K., Inagaki, T., Hara, T., Tanaka, T., Joti, Y., Koyama, T., Nakajima, K., Ohashi, H., Senba, Y., Togashi, T., Tono, K., Yamaga, M., Yumoto, H., Yabashi, M., Tanaka, H. & Ishikawa, T. (2018). *J. Synchrotron Rad.* **25**, 282–288.
- Rackstraw, D. S., Cricosta, O., Vinko, S. M., Barbrel, B., Burian, T., Chalupsky, J., Cho, B. I., Chung, H. K., Dakovski, G. L., Engelhorn, K., Hájková, V., Heimann, P., Holmes, M., Juha, L., Krzywinski, J., Lee, R. W., Toleikis, S., Turner, J. J., Zastraub, U. & Wark, J. S. (2015). *Phys. Rev. Lett.* **114**, 1–5.
- Rohringer, N., Ryan, D., London, R. A., Purvis, M., Albert, F., Dunn, J., Bozek, J. D., Bostedt, C., Graf, A., Hill, R., Hau-Riege, S. P. & Rocca, J. J. (2012). *Nature*, **481**, 488–491.
- Schlötter, W. F., Turner, J. J., Rowen, M., Heimann, P., Holmes, M., Krupin, O., Messerschmidt, M., Moeller, S., Krzywinski, J., Souflis, R., Fernández-Perea, M., Kelez, N., Lee, S., Coffee, R., Hays, G., Beye, M., Gerken, N., Sorgenfrei, F., Hau-Riege, S., Juha, L., Chalupsky, J., Hajkova, V., Mancuso, A. P., Singer, A., Yefanov, O., Vartanyants, I. A., Cadenazzi, G., Abbey, B., Nugent, K. A., Sinn, H., Lning, J., Schaffert, S., Eisebitt, S., Lee, W. S., Scherz, A., Nilsson, A. R. & Wurth, W. (2012). *Rev. Sci. Instrum.* **83**, 043107.
- Shintake, T., Tanaka, H., Hara, T., Tanaka, T., Togawa, K., Yabashi, M., Otake, Y., Asano, Y., Bizen, T., Fukui, T., Goto, S., Higashiyama, A., Hiroto, T., Hosoda, N., Inagaki, T., Inoue, S., Ishii, M., Kim, Y., Kimura, H., Kitamura, M., Kobayashi, T., Maesaka, H., Masuda, T., Matsui, S., Matsushita, T., Maréchal, X., Nagasano, M., Ohashi, H., Ohata, T., Ohshima, T., Onoe, K., Shirasawa, K., Takagi, T., Takahashi, S., Takeuchi, M., Tamásaku, K., Tanaka, R., Tanaka, Y., Tanikawa, T., Togashi, T., Wu, S., Yamashita, A., Yanagida, K., Zhang, C., Kitamura, H. & Ishikawa, T. (2008). *Nat. Photon.* **2**, 555–559.
- Takei, Y. & Mimura, H. (2017). *J. Jpn Soc. Precision Eng.* **83**, 245–250.
- Tamásaku, K., Shigemasa, E., Inubushi, Y., Inoue, I., Osaka, T., Katayama, T., Yabashi, M., Koide, A., Yokoyama, T. & Ishikawa, T. (2018). *Phys. Rev. Lett.* **121**, 083901.
- Tamásaku, K., Shigemasa, E., Inubushi, Y., Katayama, T., Sawada, K., Yumoto, H., Ohashi, H., Mimura, H., Yabashi, M., Yamauchi, K. & Ishikawa, T. (2014). *Nat. Photon.* **8**, 313–316.
- Tschentscher, T., Bressler, C., Grünert, J., Madsen, A., Mancuso, A., Meyer, M., Scherz, A., Sinn, H. & Zastraub, U. (2017). *Appl. Sci.* **7**, 592.
- Yoneda, H., Inubushi, Y., Nagamine, K., Michine, Y., Ohashi, H., Yumoto, H., Yamauchi, K., Mimura, H., Kitamura, H., Katayama, T., Ishikawa, T. & Yabashi, M. (2015). *Nature*, **524**, 446–449.
- Yoneda, H., Inubushi, Y., Tanaka, T., Yamaguchi, Y., Sato, F., Morimoto, S., Kumagai, T., Nagasano, M., Higashiyama, A., Yabashi, M., Ishikawa, T., Ohashi, H., Kimura, H., Kitamura, H. & Kodama, R. (2009). *Opt. Express*, **17**, 23443.
- Yoneda, H., Inubushi, Y., Yabashi, M., Katayama, T., Ishikawa, T., Ohashi, H., Yumoto, H., Yamauchi, K., Mimura, H. & Kitamura, H. (2014). *Nat. Commun.* **5**, 1–5.
- Yumoto, H., Mimura, H., Koyama, T., Matsuyama, S., Tono, K., Togashi, T., Inubushi, Y., Sato, T., Tanaka, T., Kimura, T., Yokoyama, H., Kim, J., Sano, Y., Hachisu, Y., Yabashi, M., Ohashi, H., Ohmori, H., Ishikawa, T. & Yamauchi, K. (2012). *Nat. Photon.* **7**, 43–47.